



WORLD  
METEOROLOGICAL  
ORGANIZATION



# GLOBAL SEASONAL CLIMATE UPDATE

TARGET SEASON: June-July-August 2024

Issued: 20 May 2024



## Summary

During February-April 2024, the Pacific Niño sea-surface temperature (SST) index in the eastern Pacific (Niño 1+2) returned to near-normal. The other three indices in the central Pacific were above-normal, but they declined in their amplitude compared to the previous months. The observed SST conditions in the equatorial Pacific were characterized by a continued weakening of El Niño state. The observed Indian Ocean Dipole (IOD) was above-normal. Both the North Tropical Atlantic (NTA) and South Tropical Atlantic (STA) SST index were much above-normal and reflected widespread warmth in the tropical Atlantic. In general, the observed SST anomalies in global oceans were positive<sup>1</sup>.

Above-normal sea-surface temperature anomalies in the Niño 3.4 and Niño 3 regions are predicted to decline during June-August 2024, and possibly cool to weak La Niña conditions by late in 2024. Farther west in the Niño 4 region, the sea-surface temperature anomaly is predicted to be near-normal. The strength of the Indian Ocean Dipole (IOD) index is predicted to return to near normal. In the equatorial Atlantic, SSTs are predicted to be above-normal in both the northern (NTA) and the southern (STA) areas during the season.

Consistent with the anticipated persistence of widespread above-normal sea-surface temperatures in all areas outside of the near-equatorial eastern Pacific Ocean, there is widespread prediction of above-normal temperatures over almost all land areas. Exceptions to this widespread warmth are South America south of about 30° S, the south-western coast of North America and in the vicinity of the Bering Sea. Extensive areas of large increases in probabilities for above-normal temperatures include almost all of Africa, and within about 45° N of the equator over Europe, and Asia, and within about 25° over Northern, Central and South America and the Caribbean. Australia, New Zealand, and most of the islands in the South Pacific have moderate to strongly increased probabilities for above-normal temperatures. North of about 60° N, North America, Europe and Asia have weak to moderately increased probabilities for above-normal temperature. South America south of about 30° S is the only extensive land area with no increase in the probability of above-normal temperature - there is no clear signal in this area. However, in coastal areas of southern South America and extending north along the west coast to just north of the equator and into the eastern Pacific below-normal temperatures are expected, consistent with the predicted emergence of La Niña conditions.

Predictions for rainfall are, in part, consistent with the canonical impacts of the early stages of La Niña conditions, which are expected to emerge mid-year. Below-normal rainfall is predicted over a narrow band along or just north of the equator from 150° E extending eastward to the southern region of Central America. There are additional bands of predicted dry conditions spanning the width of the Pacific at about 20° latitude in both Hemispheres. The Northern Hemisphere band extends into north-western Central America and the south-western part of North America. The Southern Hemisphere band is more extensive, expanding over almost the entire South America south of the equator and then across the South Atlantic. Another dry area in the southern Atlantic crosses the southernmost part of Africa and covers Madagascar, terminating at about 60° E, but reappearing over the south-western and southern parts of the Maritime continent. There are separate patchy areas of predicted increased probabilities of below-normal rainfall over parts of Europe. Much of central and eastern Africa have increased probabilities for above-normal rainfall. This wet area expands over much of the Middle East and northern Indian Ocean and some parts of South Asia. It extends along the equator through the Maritime continent and then in a narrow band immediately south of the equator as far as the central Pacific. There are strong indications of above-normal rainfall in an area centred over the Caribbean extending westward into a small area of the eastern Pacific, and eastward to the southwest coast of Africa. Weakly enhanced probabilities for above-normal rainfall are also indicated over parts of East Asia, the east coast of North America, and Greenland, as well as over much of the Southern Ocean. However, most of Asia, Europe, North America, North and West Africa, Australia and New Zealand have no clear signal. Areas in Africa where normal rainfall is indicated as the most likely outcome are generally arid at this time of year.

---

<sup>1</sup> See <https://www.cpc.ncep.noaa.gov/products/people/mchen/AttributionAnalysis/images/Attribution202404.pdf>

## Surface Air Temperature, JJA 2024

## Rainfall, JJA 2024

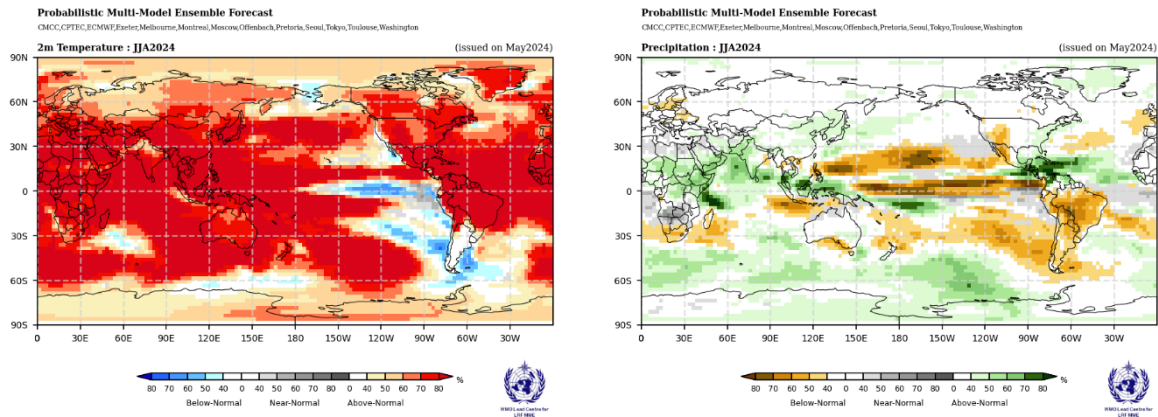


Figure 1. Probabilistic forecasts of surface air temperature and rainfall for the season June-August 2024. The tercile category with the highest forecast probability is indicated by shaded areas. The most likely category for below-normal, above-normal, and near-normal is depicted in blue, red, and grey shadings respectively for temperature, and orange, green and grey shadings respectively for rainfall. White areas indicate equal chances for all categories in both cases. The baseline period is 1993-2009.

### 1. Observations: February-April 2024

In the following sections, observed temperature and rainfall patterns for the previous season are discussed. For more detailed information about regional and local climate anomalies, the reader is referred to the concerned WMO Regional Climate Centres (RCCs) or RCC Networks, listed in Section 5.

#### 1.1 Large-scale sea-surface temperature (SST) indices

During February-April 2024, the Pacific Niño sea-surface temperature (SST) index in the eastern Pacific (Niño 1+2) returned to near-normal. The other three indices in the central Pacific were above-normal, but they declined in their amplitude compared to the previous months. The observed SST conditions in the equatorial Pacific were characterized by a continued weakening of El Niño state. The observed Indian Ocean Dipole (IOD) was above-normal. Both the North Tropical Atlantic (NTA) and South Tropical Atlantic (STA) SST index were much above-normal and reflected widespread warmth in the tropical Atlantic. In general, the observed SST anomalies in global oceans were positive<sup>1</sup>.

Month	Niño 1+2	Niño 3	Niño 4	Niño 3.4	IOD	NTA	STA
February 2024	0.9	1.5	1.2	1.5	0.3	1.3	1.2
March 2024	0.3	1.0	0.9	1.2	0.5	1.5	1.4
April 2024	0.1	0.6	0.8	0.8	0.3	1.5	1.3
February-April 2024	0.4	1.0	1.0	1.2	0.4	1.4	1.3

Table 1. Large-scale oceanic indices (°C). Anomalies are with respect to the 1991-2020 average. (Source: U.S. Climate Prediction Center)

## 1.2 Observed temperature

Over land, temperature anomalies for February-April 2024 were generally above-normal with small regions of below-normal temperatures interspersed in between (Figure 2, top). In the northern hemisphere, the largest positive land-temperature anomalies occurred over the eastern half and northern regions of North America, Greenland, and eastern Europe. In the southern hemisphere positive land-temperature anomalies generally occurred in South America, South Africa (except for the coastal regions of Central Africa adjacent to the Gulf of Guinea), and New Zealand. Patchy regions of negative temperature anomaly were observed along the western coastal regions of North and South America, western regions of Eastern Asia, Northern Asia, interior regions of Western Africa, and Australia.

Over the oceans, in the equatorial Pacific extending from the Date Line all the way to the western coastal regions of South America and extending further north along the coast of Central America, above-normal temperature anomalies occurred. These temperature anomalies reflected the decaying phase of El Niño. In the extratropical southern Pacific Ocean between (60°-30° S, 150°-60° W), below average temperatures were observed. Temperature anomalies in the northern Pacific along 45° N and in the southern Pacific along 45° S (extending to 120° W) were positive. In the Indian Ocean, warm temperatures occurred throughout the ocean basin with larger values in the western Indian Ocean. The east-west temperature gradient was consistent with a positive phase of the Indian Ocean Dipole. Temperatures in the Atlantic Ocean were generally warm with largest positive values between 30° S-30° N.

Over land, warm extremes (exceeding all seasonal mean temperatures observed during 1991-2020), occurred over South America in an elongated north-south band along 60° W, eastern regions of equatorial Africa, and parts of eastern Europe. More extensive regions of warm extremes occurred over the oceans and included the Atlantic Ocean between 30° S - 30° N, and in the Southern Ocean along 60° S between the Date Line and 140° W and between 30° W - 30° E. No systematic regions with cold extremes were observed.

## 1.3 Observed rainfall

For February-April 2024, the rainfall anomalies in the equatorial Pacific reflected a decaying El Niño state with a narrow band of above-average rainfall extending eastward from the Date Line just north of the equator (Figure 3, top panel). West of the Date Line, above-average rainfall anomalies extended to 120° E where a branch of above-average rainfall extended south-eastward across the south Pacific towards South America. In the eastern Pacific, positive rainfall anomalies along the equator were flanked by below-normal rainfall. The northern branch of below-normal rainfall extended westward towards the South China Sea and crossed southeast Asia into the Bay of Bengal. Above-normal rainfall anomalies were observed in the equatorial western Indian Ocean while below-normal rainfall anomalies occurred in the eastern Indian Ocean, a pattern consistent with the positive phase of the IOD. Below-normal rainfall anomalies dominated the equatorial Atlantic and extended northward towards Greenland. In the southern Atlantic below the equator, above-normal rainfall anomalies were observed. Similar to the Atlantic Ocean, rainfall anomalies in the North Pacific were dominated by below-normal conditions.

Over land, negative rainfall anomalies dominated South America (except for a narrow coastal band along the south and northeast). Below-normal rainfall anomalies also occurred in western parts of Africa below the equator while above-normal rainfall occurred towards the east. Above-normal rainfall anomalies occurred over western Europe and western parts of southern Europe. Above-normal rainfall was also observed over the Arabian Peninsula, coastal and adjacent interior regions of East Asia, the Maritime continent, and northeast region of Australia. Below-normal rainfall dominated Greenland and North America north of 45° N.

Patchy regions of dry extremes (drier than all seasonal mean rainfall observed during 1991-2020) occurred over parts of south-eastern Greenland, eastern Indian Ocean below the equator, Southern Ocean below Australia, southern Pacific near 50° S, 120° W. Similarly, a few patchy regions of wet extremes were observed in the western equatorial Indian Ocean, south-eastern parts of the Arabian Peninsula. In general, regions with coherent wet and dry extremes were absent.

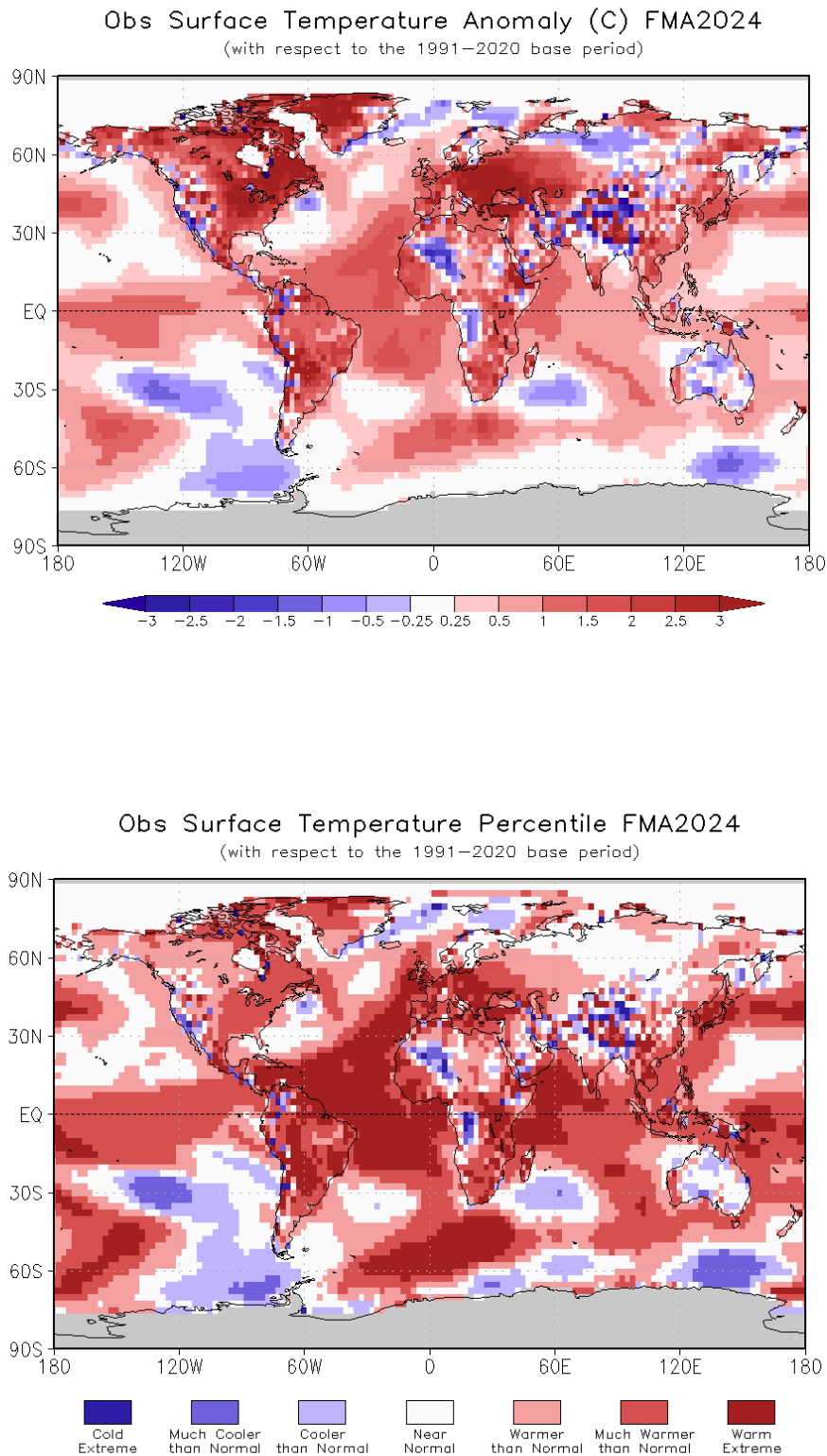


Figure 2. Observed February–April 2024 near-surface temperature anomalies relative to 1991–2020 (top). The *Cooler than Normal*, *Near Normal*, and *Warmer than Normal* shadings on the percentile map (bottom) indicate that seasonal mean anomalies were in the bottom, middle, and upper tercile of the 1991–2020 distribution, respectively. Regions with anomalies in the lowest and highest decile (or 10%) of the distribution are marked as *Much Cooler than Normal* and *Much Warmer than Normal*, respectively. The *Cold Extreme* and *Warm Extreme* shadings indicate that the anomalies exceeded the coldest and warmest temperature values of the 1991–2020 period for the season. Grey shading indicates areas where observational analysis was not available. (Source: U.S. Climate Prediction Center).

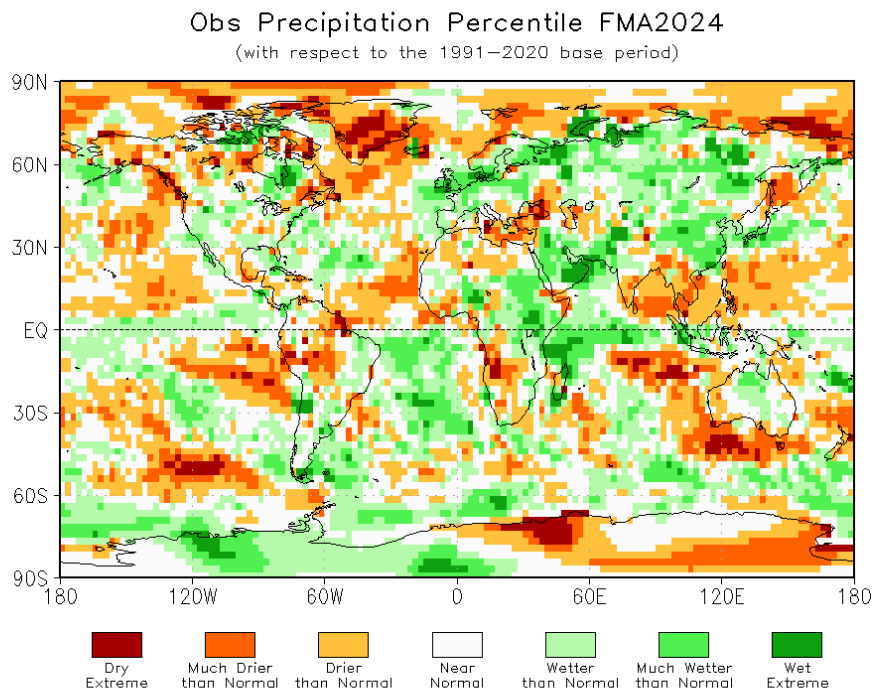
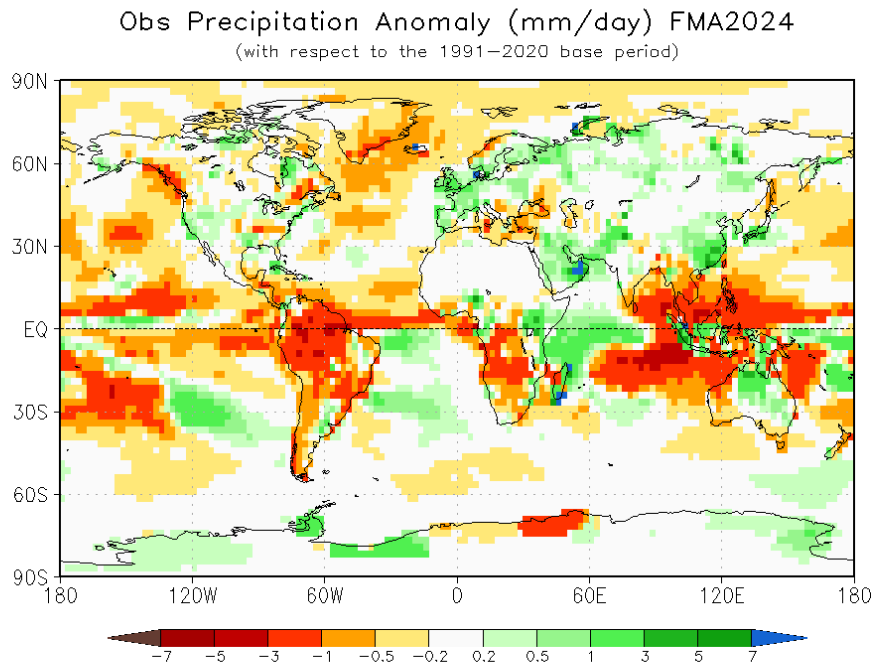


Figure 3. Observed rainfall anomalies for February-April 2024, relative to 1991-2020 base period (top). The *Drier than Normal*, *Near Normal* and *Wetter than Normal* shadings on the percentile map (bottom) indicate that seasonal mean anomalies were in the bottom, middle, and upper tercile of the 1991-2020 distribution, respectively. Regions with anomalies in the lowest and highest decile (or 10%) of the distribution are marked as *Much Drier than Normal* and *Much Wetter than Normal*, respectively. The *Dry Extreme* and *Wet Extreme* shadings indicate that the anomalies exceeded the driest and wettest values of the 1991-2020 period for the season. (Source: U.S. Climate Prediction Center).

## 2. Potential evolution of the state of the climate over the next three months (June-August 2024)

### 2.1 Large-scale SST-based indices, June-August 2024

Month	Nino 1+2	Nino 3	Nino 4	Nino3.4	IOD	NTA	STA
<b>June 2024</b>	-0.3±0.3	-0.2±0.4	0.6±0.2	0.1±0.3	0.6±0.2	1.1±0.2	0.9±0.2
<b>July 2024</b>	-0.5±0.4	-0.3±0.4	0.3±0.3	-0.1±0.4	0.6±0.2	0.9±0.2	0.8±0.2
<b>August 2024</b>	-0.5±0.4	-0.4±0.4	0.1±0.3	-0.3±0.4	0.5±0.4	0.8±0.2	0.7±0.2
<b>June-August 2024</b>	-0.4±0.4	-0.3±0.4	0.4±0.3	-0.1±0.4	0.6±0.3	1.0±0.2	0.8±0.2

Table 2: Multi-model forecasts for oceanic indices (°C), with standard deviation. Values are the equal-member-weighting average of those derived, using each GPC model's own hindcast climate mean, from the GPCs supplying SST forecasts (GPC Beijing, CMCC, ECMWF, Exeter, Melbourne, Montreal, Offenbach, Seoul, Tokyo, Toulouse, Washington). The standard deviation is calculated on all ensemble members. The latitude/longitude bounds of the regions are given in the supplementary information section.

Above-normal sea-surface temperature anomalies in the Niño 3.4 and Niño 3 regions are predicted to decline during June-August 2024, and possibly cool to weak La Niña conditions by late in 2024. Farther west in the Niño 4 region, the sea-surface temperature anomaly is predicted to be near-normal. The strength of the Indian Ocean Dipole (IOD) index is predicted to return to near normal. In the equatorial Atlantic, SSTs are predicted to be above-normal in both the northern (NTA) and the southern (STA) areas during the season.

### 2.2 Predicted temperature, June-August 2024

For information on the construction of the multi-model forecast maps, refer to the supplementary information section. (Note: Maps indicating forecast consistency among GPC models are available in the supplementary information<sup>2</sup>).

<sup>2</sup> File with supplementary information can be downloaded from [https://ftp.cpc.ncep.noaa.gov/mingyue/GSCUWMO/Forecasts/GSCU\\_JJA2024\\_supplementary\\_info\\_LC-LRFMME.docx](https://ftp.cpc.ncep.noaa.gov/mingyue/GSCUWMO/Forecasts/GSCU_JJA2024_supplementary_info_LC-LRFMME.docx)

### Probabilistic Multi-Model Ensemble Forecast

CMCC, CPTEC, ECMWF, Exeter, Melbourne, Montreal, Moscow, Offenbach, Pretoria, Seoul, Tokyo, Toulouse, Washington

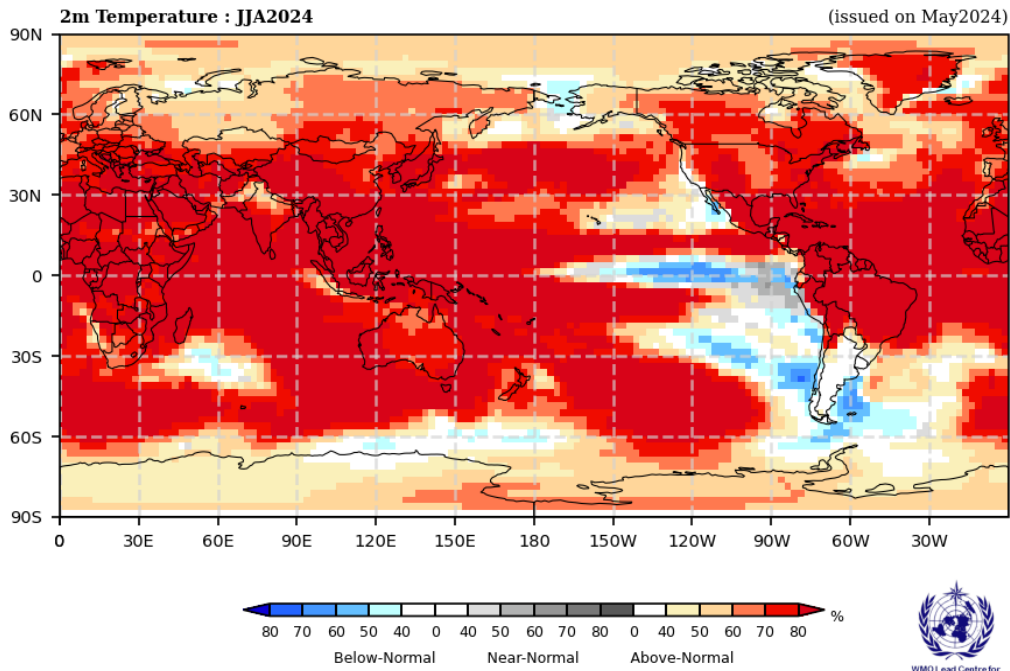


Figure 4. Probabilistic forecasts of surface air temperature for June-August 2024. The tercile category with the highest forecast probability is indicated by shaded areas. The most likely category for below-normal, above-normal, and near-normal is depicted in blue, red, and grey shadings, respectively. White areas indicate equal chances for all categories in both cases. The baseline period is 1993-2009. Figure is generated by The WMO Lead Centre for Long-Range Forecast Multi-Model Ensemble.

Consistent with the anticipated persistence of widespread above-normal sea-surface temperatures in all areas outside of the near-equatorial eastern Pacific Ocean, there is widespread prediction of above-normal temperatures over almost all land areas. Exceptions to this widespread warmth are South America south of about 30° S, the southwestern coast of North America and in the vicinity of the Bering Sea. Extensive areas of large increases in probabilities for above-normal temperatures include almost all of Africa, and within about 45° N of the equator over Europe, and Asia, and within about 25° over Northern, Central and South America and the Caribbean. Australia, New Zealand, and most of the islands in the South Pacific have moderate to strongly increased probabilities for above-normal temperatures. North of about 60° N, North America, Europe and Asia have weak to moderately increased probabilities for above-normal temperature. South America south of about 30° S is the only extensive land area with no increase in the probability of above-normal temperature - there is no clear signal in this area. However, in coastal areas of southern South America and extending north along the west coast to just north of the equator and into the eastern Pacific below-normal temperatures are expected, consistent with the predicted emergence of La Niña conditions.

RA I (Africa): Enhanced probabilities of above-normal temperatures are indicated over all of mainland Africa and Madagascar. The probability increases are strong everywhere, but model consistency is strong only over the southern part of West Africa. Elsewhere, model consistency is moderate. Immediately to the southeast of Madagascar there is an area of weakly increased probabilities for below-normal temperatures, but model consistency is weak.

RA II (Asia): Enhanced probabilities for above-normal temperatures are indicated over all of mainland Asia, with higher probabilities south of 45° N, but the model consistency is high only in the south and southeast. North of this region, enhancement in the probability for above-normal temperatures is moderate, or, between about 30° and 90° E is weak. Smaller areas of weakly enhanced probabilities for above-normal temperature are also indicated in South Asia at about 30° N, 75° E, and in the extreme south-western part of the Maritime continent. In the far northeast, in the vicinity of the Bering Sea, the probabilities for below-normal temperature are weakly enhanced.



RA III (South America): Strongly enhanced probabilities for above-normal temperatures are indicated over South America north of about 30° S with the exception of the narrow Pacific coastal strip. Model consistency is very high in this region. Further south, there is no clear indication for a signal except along narrow coast areas where below-normal temperature is predicted.

RA IV (North America, Central America, and the Caribbean): There are enhanced probabilities for above-normal temperatures over almost all of Central and North America and the Caribbean, with the exception of the narrow Pacific coast, the area near the Bering Sea, and between the Hudson Bay and Greenland. The probabilities for above-normal temperatures are strongest over Central America and the Caribbean south of about 30° N, and moderate to strong over most of the rest of the region, but becoming weak in the far northwest and between Greenland and mainland North America. Model consistency is high south of about 40° N, and moderate to high over most of the inland areas. Along the Pacific coast between about 15° and 40° N, the signal is weak.

RA V (Southwest Pacific): Widespread and strongly enhanced probabilities for above-normal temperatures are predicted throughout the region and the model consistency is mostly high. This area of predicted warmth extends to about Date Line, marking the western edge of a narrow tongue of predicted below-normal temperatures associated with the predicted La Nina. Probabilities and model consistency weaken a little over northern Australia and in the vicinity of New Zealand, as well as immediately south and southwest of the Maritime Continent. The area of warmth extends into the eastern Pacific in four prongs. One extension is a narrow band at about 10° N that connects all the way to Central America. North of this area is a band between about 30 ° and 60 ° N that weakens towards North America. A third extension at about 10° S reaches about 120° W, and the southernmost extension approaches 90° W and 60° S. These bands are separated by smaller areas of predicted colder than average temperatures, the strongest of which is along the equator, and is the most extensive and strongest in the South Pacific.

RA VI (Europe): The probabilities for above-normal temperatures are increased over all of Europe with highest probabilities south of about 45° N. The model-to-model consistency is patchy, but mostly weak to moderate.

### 2.3 Predicted rainfall, June-August 2024

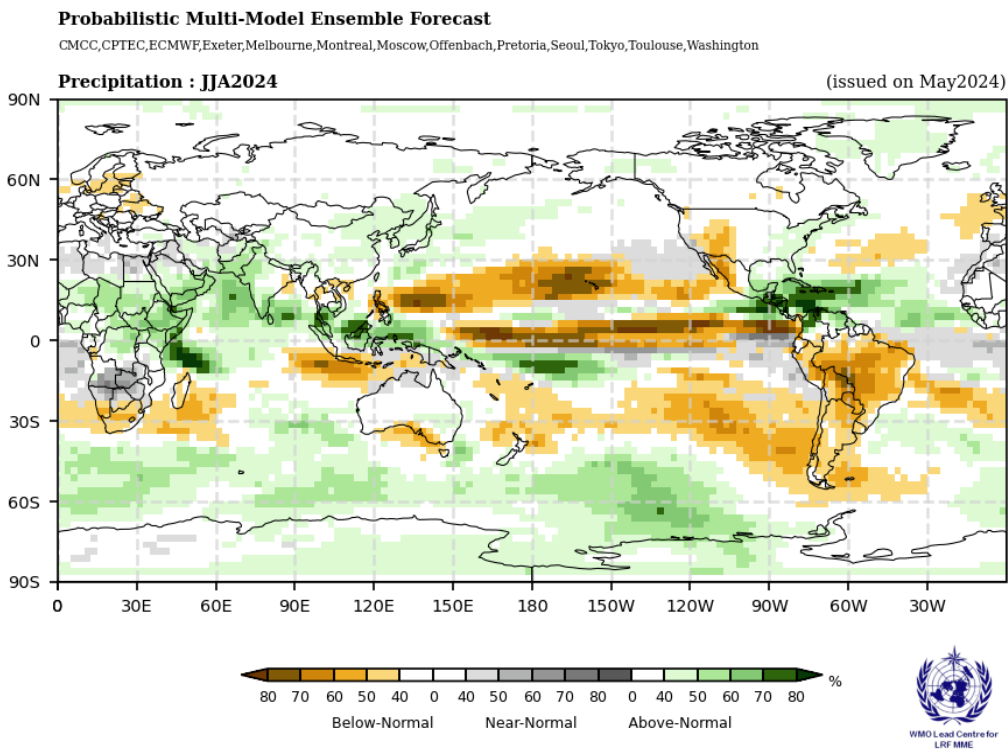


Figure 5. Probabilistic forecasts of rainfall for the season for June-August 2024. The tercile category with the highest forecast probability is indicated by shaded areas. The most likely category for below-normal, above-normal, and near-normal is depicted in orange, green and grey shadings, respectively. White areas indicate equal chances for all categories in both cases. The baseline period is 1993-2009. Figure is generated by The WMO Lead Centre for Long-Range Forecast Multi-Model Ensemble.

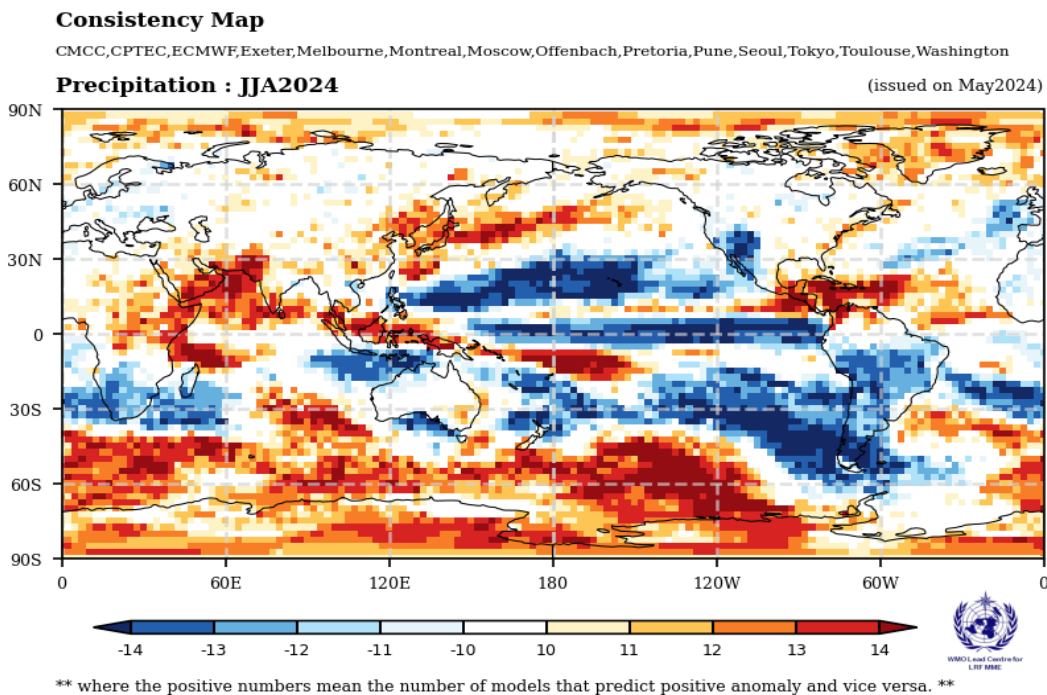
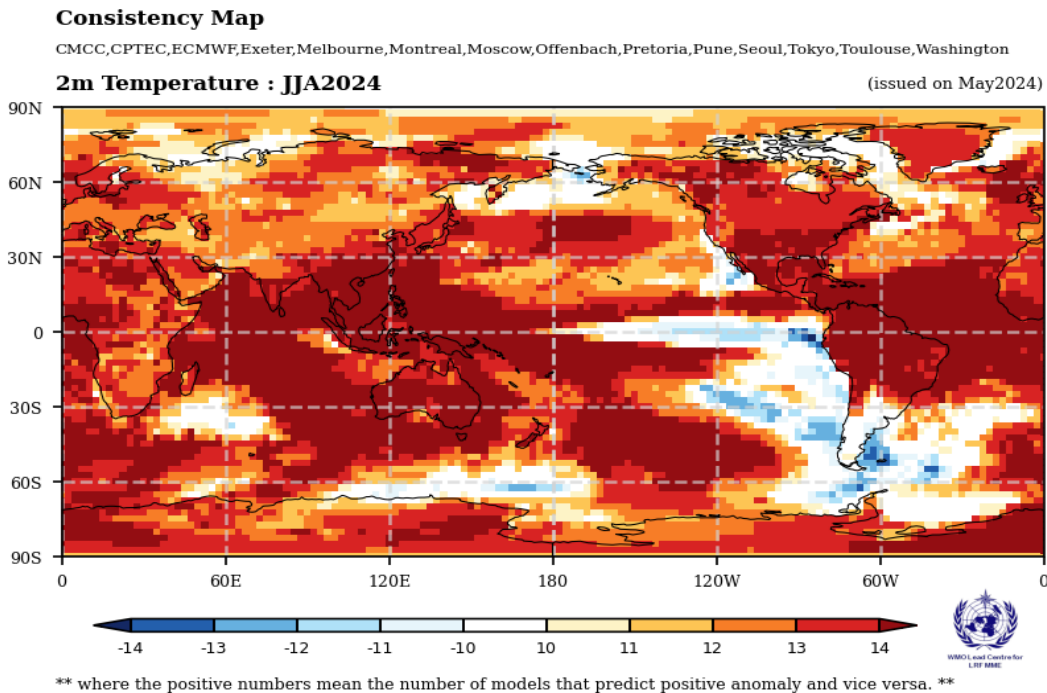


Figure 6. Consistency maps for sign of ensemble mean anomalies for the seasonal mean of June-August 2024 for surface air temperature (top) and rainfall (bottom) from different model forecasts. The consistency map is constructed using the following procedure: At each grid point the number of models with positive or negative anomaly is counted and the number that is larger is plotted on the map. For example, if the number of models with positive (negative) anomaly is larger then the count is plotted on the map using the red (blue) scale. Darker (lighter) colours imply that there is a higher (lower) consistency in the sign of anomalies between models.

Predictions for rainfall are, in part, consistent with the canonical impacts of the early stages of La Niña conditions, which are expected to emerge mid-year. Below-normal rainfall is predicted over a narrow band along or just north

of the equator from 150° E extending eastward to the southern region of Central America. There are additional bands of predicted dry conditions spanning the width of the Pacific at about 20° latitude in both Hemispheres. The Northern Hemisphere band extends into north-western Central America and the south-western part of North America. The Southern Hemisphere band is more extensive, expanding over almost the entire South America south of the equator and then across the South Atlantic. Another dry area in the southern Atlantic crosses the southernmost part of Africa and covers Madagascar, terminating at about 60° E, but reappearing over the south-western and southern parts of the Maritime continent. There are separate patchy areas of predicted increased probabilities of below-normal rainfall over parts of Europe. Much of central and eastern Africa have increased probabilities for above-normal rainfall. This wet area expands over much of the Middle East and northern Indian Ocean and some parts of South Asia. It extends along the equator through the Maritime continent and then in a narrow band immediately south of the equator as far as the central Pacific. There are strong indications of above-normal rainfall in an area centred over the Caribbean extending westward into a small area of the eastern Pacific, and eastward to the southwest coast of Africa. Weakly enhanced probabilities for above-normal rainfall are also indicated over parts of East Asia, the east coast of North America, and Greenland, as well as over much of the Southern Ocean. However, most of Asia, Europe, North America, North and West Africa, Australia and New Zealand have no clear signal. Areas in Africa where normal rainfall is indicated as the most likely outcome are generally arid at this time of year.

RA I (Africa): Between about 10° S and 25° N and east of 0°, there are increased probabilities for above-normal precipitation. The signal strengthens towards the east and is strongest to the north of Madagascar. Model consistency is weak to moderate, but also strengthens over the Greater Horn of Africa. Above-normal precipitation also has increased probabilities in the far southwestern part of West Africa. South of about 20° S, and over Madagascar and the southwest Indian Ocean, below-normal rainfall probabilities are increased, although most of this region experiences its dry season at this time of year. Similarly, with increased probabilities of normal rainfall in southern Africa as well as across much of North Africa are primarily a reflection for the dry season.

RA II (Asia): Strong rainfall signals over Asia are generally confined to the more southerly latitudes, where there is a large somewhat discontinuous area of increased probabilities for above-normal rainfall. The probabilities and model consistency are highest in the Arabian Peninsula, and nearby parts of southwest Asia, and continuing north of the equator over the far southern part of Southeast Asia and into the central Maritime Continent. This same area extends weakly and patchily into East Asia where model consistency is moderate, but probabilities are still low. Elsewhere over mainland Asia there is no clear signal. The southernmost part of the Maritime Continent has increased chances of below-normal precipitation, and model consistency is high. There is also an area of predicted dryness extending from the Philippines eastward across the Pacific toward North America. Probabilities and model consistency are strong east of about 125° E.

RA III (South America): Almost all of South America has increased probabilities for below-normal precipitation. The probabilities are highest in the central interior, but model consistency is strongest in the south. North of the equator there is a sharp transition to an area with increased probabilities of above-normal precipitation. The probabilities of wet conditions are high here, and model consistency is strong. Along the Pacific coast, from north of the equator to about 20° S, near-normal precipitation is the most likely outcome, but model consistency is weak.

RA IV (North America, Central America, and the Caribbean): Probabilities for above-normal rainfall are strongly enhanced over an area that extends from southern Central America over most of the Caribbean and northernmost parts of South America. Model consistency is strong. This wet zone extends with greatly diminished strength and very weak model consistency along the eastern parts of North America. To the far south-east is a zone of expected dry conditions that clips the southernmost part of Central America. However, there is a larger of predicted dry conditions that includes northwestern Central America and the southwestern part of North America. Both these dry areas have moderate to strong model consistency. Weak indications of increased probabilities for wet conditions are indicated over Greenland, and to a lesser extent in the northwestern part of North America, but model consistency is weak. Elsewhere, over the bulk of North America, there is no clear signal.

RA V (Southwest Pacific): Probabilities for above-normal rainfall are strongly enhanced over a near-equatorial band area that extends from the central Maritime Continent to just south of the equator east of 150° E as far as 150° W. The band is narrow, but probabilities are high and model consistency is strong. To the south there is a discontinuous and generally weaker zone of below-normal rainfall. This area is moderately strong to the northwest of Australia, weakening to the north of Australia, and then reappears east of about 160° E where it extends as far as South America centered along about 30°S. The probabilities throughout this area are moderate to strong, and model consistency is high. The dry area over the Pacific forms part of a complex zones of contrasting rainfall anomalies across the entire Pacific Ocean. East of 150° E the equatorial band is predicted to be dry, becoming near-normal towards South America. This narrow equatorial tongue is bracketted by a very narrow strip of both to the north and south, where the signal weakens or becomes near-normal or even above-normal. Further away from the equator again, along about 20° N and 30° S below-normal rainfall is again predicted. This band is strongest in the North Pacific, most notably between the Date Line and 150° W. Along the south coast of Australia an area of dryness is also indicated, Probabilities are low here, model consistency is high. There is a weaker indication of above-normal rainfall in over south-western Australia, but both the probabilities and the model consistency are low. Signals are weak over the rest of Australia and over New Zealand.

RA VI (Europe): Most of Europe has no clear signal, although there are a few patchy areas of weakly enhanced probabilities of below-normal rainfall. Model consistency is weak.

### 3. Latest updates for monitoring and prediction information

Each month, the latest updates for the real-time monitoring and seasonal mean predictions included in GSCU can be found at:

Monitoring:

<https://ftp.cpc.ncep.noaa.gov/mingyue/GSCUWMO/>

Predictions:

[www.wmolc.org/board/downloadExt?fn=WMOLC\\_T2M.png](http://www.wmolc.org/board/downloadExt?fn=WMOLC_T2M.png)

#### 4. How to use the Global Seasonal Climate Update

The GSCU is intended as guidance for RCCs, Regional Climate Outlook Forums (RCOFs) and National Meteorological and Hydrological Services (NMHSs). It does not constitute an official forecast for any region or nation. Seasonal outlooks for any region or nation should be obtained from the relevant RCCs (see below for contact details) or NMHS.

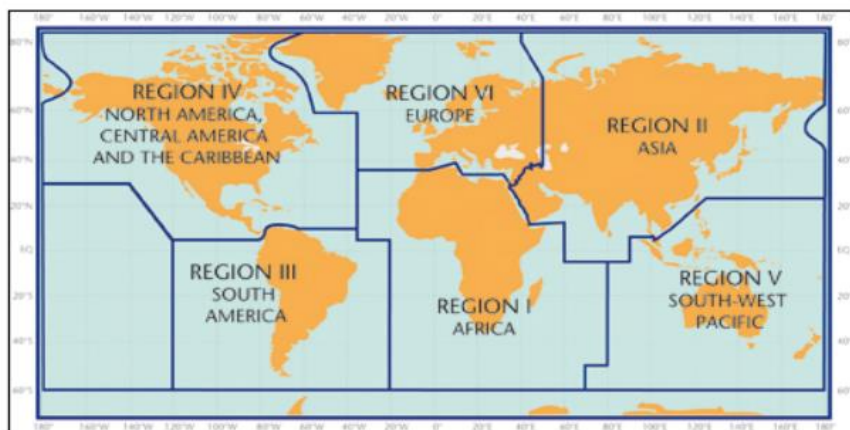
Figure 4 shows the spatial pattern of seasonal mean surface air temperature forecast probabilities. Probabilities are calculated for the average temperature for the season being in the highest third (above-normal or warm), middle third (normal) or lowest third (below-normal or cold) ranges of the baseline record (1993-2009) at each location. Colour code is indicated only for the category that has the highest probability of occurrence. For example, for regions highlighted in red, the most likely forecast category for seasonal mean surface air temperature to occur is warmer than normal. Similarly, the blue colour highlights regions where the seasonal mean surface air temperature forecast indicates the colder than normal category as most likely, while grey colour highlights regions where the seasonal mean temperature forecast indicates the near normal category as most likely. Deeper shades of respective colours highlight increasing probability for the seasonal mean temperature to be in the indicated category. White areas indicate equal chances for all categories.

A particular colour does not assure that the seasonal mean temperature is “certain” to be observed in the most likely forecast category that is shown, but rather its probability of being in that category. As a consequence, the observed seasonal mean temperatures have a non-negligible probability to be observed in a category different from the category indicated on the map as most likely. Users need to take the probabilistic nature of seasonal forecasts into account when making decisions. It should also be noted that the absolute values for the surface air temperature corresponding to the definitions of the above normal (warm), normal or below normal (cold) categories depend on the climatology (historical information) at the location, and therefore, is location dependent.

The interpretation of the probabilities for the rainfall forecast (Figure 5) is the same as that for the seasonal mean surface air temperature except that green and brown colours indicate whether the forecasted seasonal mean rainfall is most likely to be in the wet or dry category. As for surface temperature, grey colour highlights regions where the seasonal mean rainfall forecast indicates the near normal category as the most likely.

The skill of seasonal forecasts is substantially lower than that of weather timescales and skill may vary considerably with region and season. It is important to view the forecast maps together with the skill maps provided in the supplementary material.

For reference, the six WMO Regional Associations domains are depicted in the figure below.



## 5. Designated and developing WMO Regional Climate Centres and Regional Climate Centre Networks

- <https://public.wmo.int/en/our-mandate/climate/regional-climate-centres>

## 6. Resources

Sources for the graphics used in the GSCU:

- The WMO Lead Centre for Long-Range Forecast Multi-Model Ensemble (LC-LRFMME): <http://www.wmolc.org>
- WMO portal to the Global Producing Centres for Long-range Forecasts (GPCs-LRF): <https://public.wmo.int/en/programmes/global-data-processing-and-forecasting-system/global-producing-centres-of-long-range-forecasts>
- WMO portal for Regional Climate Outlook Forums <https://public.wmo.int/en/our-mandate/climate/regional-climate-outlook-products>
- International Research Institute for Climate and Society (IRI): <https://iri.columbia.edu/>
- NOAA Climate Prediction Centre (CPC): <http://www.cpc.ncep.noaa.gov> ; <https://www.cpc.ncep.noaa.gov/products/people/mchen/AttributionAnalysis/>

## 7. Acknowledgements

This Global Seasonal Climate Update was jointly developed by the WMO Infrastructure (INFCOM) and Services (SERCOM) Commissions with contributions from:

- WMO Lead Centre for Long-Range Forecast Multi-Model Ensemble (LC-LRFMME), Korea Meteorological Administration, NOAA National Centers for Environmental Prediction
- WMO Global Producing Centres for Long-Range Forecast (GPCs-LRF): GPC-Beijing (China Meteorological Administration), GPC-CPTEC (Center for Weather Forecast and Climate Studies, Brazil), GPC-ECMWF (European Center for Medium-Range Forecast), GPC-Exeter (UK Met Office), GPC- Melbourne (Bureau of Meteorology), GPC-Montreal (Meteorological Services of Canada), GPC-Moscow (Hydro meteorological Center of Russia), GPC-Offenbach Deutscher Wetterdienst), GPC-Pretoria (South African Weather Services), GPC-Seoul (Korea Meteorological Administration), GPC-Tokyo (Japan Meteorological Agency), GPC-Toulouse (Météo-France), GPC-Washington (National Centers for Environmental Prediction), GPC-CMCC (Centro Euro-Mediterraneo sui Cambiamenti Climatici), GPC-Pune (India Meteorological Department).
- International Research Institute for Climate and Society (IRI)